Protein Science (2000), *9*:145–157. Cambridge University Press. Printed in the USA.

Apoflavodoxin (un)folding followed at the residue level by NMR

CARLO P.M. VAN MIERLO,[1] JOS M.P. VAN DEN OEVER,[2] AND ELLES STEENSMA[3]

[1]Department of Biomolecular Sciences, Laboratory of Biochemistry, Wageningen University, Wageningen, The Netherlands
[2]Department of Biomolecular Sciences, Laboratory of Physical Chemistry and Colloid Science, Wageningen University, Wageningen, The Netherlands
[3]Department of Biochemistry, Uppsala University, Uppsala, Sweden

(RECEIVED August 10, 1999; FINAL REVISION October 21, 1999; ACCEPTED November 5, 1999)

Abstract

The denaturant-induced (un)folding of apoflavodoxin from *Azotobacter vinelandii* has been followed at the residue level by NMR spectroscopy. NH groups of 21 residues of the protein could be followed in a series of ^{1}H–^{15}N heteronuclear single-quantum coherence spectra recorded at increasing concentrations of guanidinium hydrochloride despite the formation of protein aggregate. These NH groups are distributed throughout the whole apoflavodoxin structure. The midpoints of unfolding determined by NMR coincide with the one obtained by fluorescence emission spectroscopy. Both techniques give rise to unfolding curves with transition zones at significantly lower denaturant concentrations than the one obtained by circular dichroism spectroscopy. The NMR (un)folding data support a mechanism for apoflavodoxin folding in which a relatively stable intermediate is involved. Native apoflavodoxin is shown to cooperatively unfold to a molten globule-like state with extremely broadened NMR resonances. This initial unfolding step is slow on the NMR chemical shift timescale. The subsequent unfolding of the molten globule is faster on the NMR chemical shift timescale and the limited appearance of ^{1}H–^{15}N HSQC cross peaks of unfolded apoflavodoxin in the denaturant range studied indicates that it is noncooperative.

Keywords: apoflavodoxin; cooperative and noncooperative unfolding; equilibrium (un)folding; guanidinium hydrochloride; molten globule; NMR; protein aggregation; residue level

Flavodoxin is an interesting model to study protein folding and stability. In contrast to most protein folds, the flavodoxin-like fold is shared by many (i.e., nine) superfamilies (Brenner, 1997). These nine superfamilies exhibit little or no sequence similarity, and comprise a broad range of unrelated proteins with different functions such as catalases, chemotactic proteins, lipases, esterases, and flavodoxins. They are all characterized by a five-stranded parallel β-sheet surrounded by α-helices at either side of the sheet. Studies on these structurally but not sequentially related proteins are pre-eminently suitable to study protein folding and stability. By studying the folding of flavodoxin, we expect to obtain a better understanding of the fundamental rules describing the folding of proteins with a flavodoxin-like fold.

Reprint requests to: Carlo P.M. van Mierlo, Department of Biomolecular Sciences, Laboratory of Biochemistry, Wageningen University, Dreijenlaan 3, NL-6703 HA Wageningen, The Netherlands; e-mail: carlo.vanmierlo@nmr.bc.wau.nl.

Abbreviations: C69A, cysteine 69 replaced by alanine; CD, circular dichroism; C_m, concentration denaturant at the midpoint of unfolding; FMN, riboflavin-5′-monophosphate; GndHCl, guanidinium hydrochloride; HSQC, heteronuclear single-quantum coherence; k_{ex}, measured amide proton exchange rate; NOESY, nuclear Overhauser effect spectroscopy.

Flavodoxins are a group of small flavoproteins that function as low-potential one-electron carriers and contain a noncovalently bound FMN cofactor (Mayhew & Tollin, 1992). The protein investigated by us is flavodoxin II from *Azotobacter vinelandii* (strain ATCC 478), henceforth designated flavodoxin. The protein consists of 179 amino acid residues and belongs to the class of "long-chain" flavodoxins (Tanaka et al., 1977). Upon removal of the flavin, apoflavodoxin is generated. Despite the removal of the FMN cofactor, large parts of the tertiary structure of holo- and apoflavodoxin are strictly conserved as is reflected among others in the identity of NMR chemical shifts (Fig. 1). Native apoflavodoxin has a stable well-ordered core, but in contrast to holoflavodoxin, its flavin binding region is shown to be flexible by NMR spectroscopy (Fig. 1) (van Mierlo et al., 1997; Steensma & van Mierlo, 1998). This flexibility is a likely prerequisite to enable the flavin to enter the interior of the apoprotein during the final stages of flavodoxin folding. Apoflavodoxin molecules are shown to rapidly dimerize via the formation of an intermolecular disulfide bond involving the sole cysteine residue at position 69. To avoid this complication, the single cysteine residue is replaced by an alanine residue (Steensma et al., 1996).

The guanidinium hydrochloride induced unfolding of apoflavodoxin is demonstrated to be reversible (van Mierlo et al., 1998).

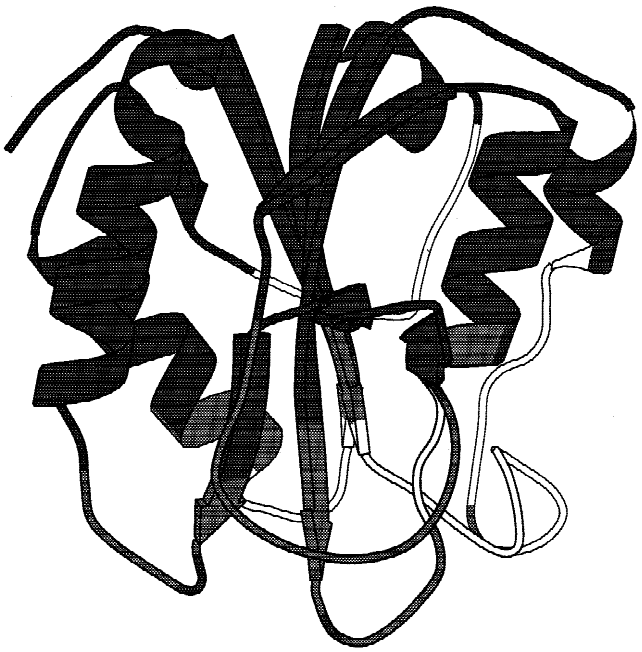

Fig. 1. MOLSCRIPT cartoon drawing (Kraulis, 1991) of the X-ray structure of *Azotobacter chroococcum* flavodoxin (Thorneley et al., 1994). The structure is gray colored according to the $^1H^{\alpha}$ chemical shift differences ($\Delta\delta$) between the holo- and the apoform of the highly homologous *A. vinelandii* C69A apoflavodoxin (Steensma & van Mierlo, 1998). The length of the α-helices and of the β-strands shown in the global fold of apoflavodoxin is determined by NMR data (Steensma & van Mierlo, 1998). Dark gray: $\Delta\delta \leq 0.1$ ppm; light gray: $\Delta\delta > 0.1$ ppm; white: residues of which the $^1H^{\alpha}$ proton could not be assigned. Dynamical exchange between different conformations occurs in the flavin binding region of the molecule that is colored light gray and white.

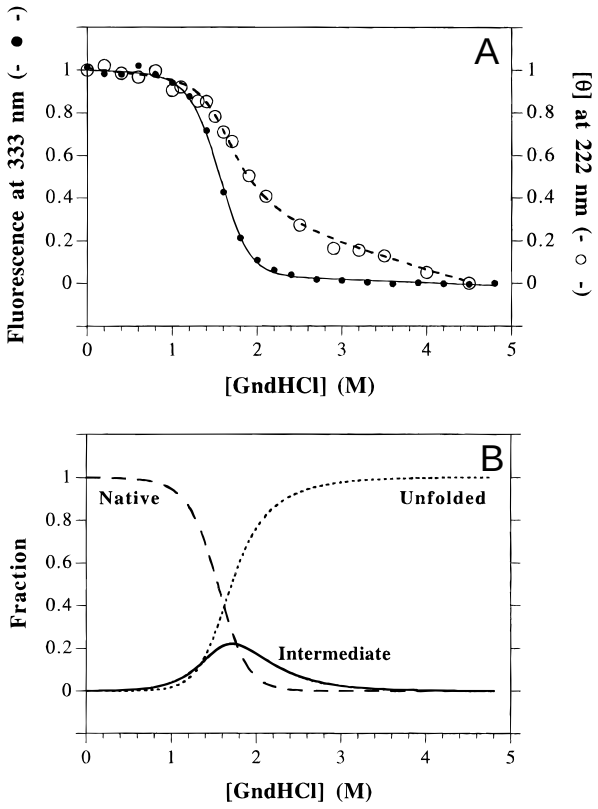

Fig. 2. Guanidinium hydrochloride unfolding profiles of C69A apoflavodoxin from *A. vinelandii* (van Mierlo et al., 1998). **A:** Profiles as measured by fluorescence at 333 nm (●) and by ellipticity at 222 nm (○). The raw data are presented, including the slopes in the baselines, except that the values are normalized to 1 and 0 for the fluorescence and the ellipticity of the native and unfolded proteins, respectively. Results of the fits for the changes in fluorescence and ellipticity calculated for a three-state transition are shown in solid and dashed lines, respectively. **B:** Simulated fractions of native (– – –), intermediate state (——), and unfolded (·-·-·) C69A apoflavodoxin molecules as a function of the concentration guanidinium hydrochloride.

Apoflavodoxin can thus fold in the absence of the FMN cofactor. The equilibrium unfolding curves obtained for apoflavodoxin as monitored by CD and fluorescence spectroscopy do not coincide (Fig. 2A). Apoflavodoxin unfolding therefore does not occur via a simple two-state mechanism. The experimental data can be described by a three-state mechanism of apoflavodoxin equilibrium unfolding (Native ↔ Intermediate ↔ Unfolded) in which a relatively stable intermediate is involved (Fig. 2B). The intermediate species lacks the characteristic tertiary structure of native apoflavodoxin as deduced from fluorescence spectroscopy, but has significant secondary structure as inferred from circular dichroism spectroscopy (van Mierlo et al., 1998). Folding intermediates with such characteristics are often referred to as molten globules (Ptitsyn, 1992).

Although valuable, fluorescence and CD spectroscopy give rather limited information about the local (un)folding of a protein. NMR spectroscopy, however, enables the study at the level of individual amino acid residues of the (un)folding of a protein (Schulman et al., 1997). The good NMR characteristics of flavodoxins (high solubility, relatively narrow line widths) allow a detailed structural characterization of these proteins in solution (van Mierlo et al., 1990a, 1990b) using a variety of heteronuclear multidimensional NMR experiments (see, e.g., Wijmenga et al., 1996, 1997). Recently ^1H, ^{13}C, and ^{15}N backbone chemical shifts of holoflavodoxin (Steensma et al., 1998) and ^1H and ^{15}N backbone chemical shifts of apoflavodoxin (Steensma & van Mierlo, 1998) have been determined. The latter enables the use of hydrogen exchange measurements that inform about local, subglobal, and global unfolding of apoflavodoxin under native conditions (Steensma & van Mierlo, 1998; van Mierlo & Steensma, 1999). It is inferred that the structured part of the apoflavodoxin molten globule coincides with the stable nucleus of native apoflavodoxin as determined by the hydrogen exchange measurements (Steensma & van Mierlo, 1998; van Mierlo et al., 1998).

The resonance assignments of apoflavodoxin enable the use of NMR spectroscopy for the investigation of the denaturant-induced (un)folding of the protein at high resolution. Comparable studies on proteins are still relatively sparse. This is in part caused by complications due to protein aggregation, which is often encountered after addition of a highly concentrated denaturant solution to the millimolar protein solutions necessary for multidimensional NMR.

In this paper, we present the results of our NMR study on the denaturant-induced (un)folding of apoflavodoxin at the level of individual amino acid residues. We show that, after a proper correction for the protein aggregation observed, the NMR data can be used to study flavodoxin folding. NH groups of 21 residues dis-

tributed throughout the whole apoflavodoxin structure are followed in a series of $^{1}H–^{15}N$ HSQC spectra recorded at increasing concentrations of guanidinium hydrochloride. The implications of the NMR results obtained for the understanding of the folding of flavodoxin are discussed.

Results

GndHCl-induced equilibrium unfolding of apoflavodoxin followed by NMR spectroscopy

Uniformly ^{15}N-labeled C69A apoflavodoxin (2.1 mM) was unfolded in an NMR tube at 298 K by controlled addition of fixed amounts of 5.41 M GndHCl. The unfolding experiments were done in 100 mM potassium pyrophosphate, pH 6.0, to be comparable to the unfolding experiments as monitored by CD and fluorescence spectroscopy (van Mierlo et al., 1998). At each concentration of denaturant used, a $^{1}H–^{15}N$ HSQC NMR spectrum was recorded. Such a spectrum serves as a fingerprint of the conformational state of a protein. The $^{1}H–^{15}N$ HSQC spectrum of native apoflavodoxin shows a nice dispersion in chemical shifts, characteristic for a folded protein (Fig. 3). Besides small buffer-concentration-dependent chemical shift changes, the spectrum is identical to the assigned spectrum of the protein in 150 mM potassium pyrophosphate, pH 6.0 (Steensma & van Mierlo, 1998). Each $^{1}H–^{15}N$ HSQC experiment was started ~0.5 h after the addition of the denaturant to the apoflavodoxin solution. This ensures that the denaturant-induced apoflavodoxin (un)folding is well at equilibrium as (un)folding the protein is complete within minutes (data not shown).

The unfolding of native apoflavodoxin monitored by cross peak volume changes in $^{1}H–^{15}N$ HSQC spectra at different stages during the equilibrium unfolding by GndHCl is shown in Figure 4. Spectra of excellent quality are obtained that demonstrates that the NMR spectroscopy of GndHCl-containing protein solutions is not significantly more difficult than spectroscopy of simple aqueous solutions (Plaxco et al., 1997).

In the $^{1}H–^{15}N$ HSQC spectra acquired at 0.20, 0.40, 0.60, 0.81, and 0.99 M GndHCl, only relatively small chemical shift changes of the $^{1}H–^{15}N$ correlations of native apoflavodoxin are observed. In the denaturant concentration range mentioned, no cross peaks appeared that could potentially correspond with an apoflavodoxin folding intermediate or the unfolded state of the protein (Fig. 4A,B). Solely a gradual decrease in the integrals of the cross peaks of native apoflavodoxin compared to the $^{1}H–^{15}N$ HSQC spectrum acquired at 0.0 M GndHCl was observed. This decrease in cross peak volume is mainly due to a reduction of the protein concentration upon addition of the denaturant and is discussed below. The absence of "non-native" $^{1}H–^{15}N$ HSQC cross peaks up to 1 M GndHCl is in good agreement with the fluorescence emission and CD data (Fig. 2).

In the spectra acquired at 1.16, 1.32, 1.46, 1.55, 1.75, and 1.95 M GndHCl, many extra cross peaks that are broadened in the ^{1}H and ^{15}N dimension are observed [see, e.g., the region (7.7–8.5 ppm (^{1}H), 115–125 ppm (^{15}N)] in Figure 4C–E. These cross peaks are most likely broadened due to exchange on the NMR chemical shift timescale between molecules with non-native conformations. In the GndHCl concentration range discussed (Fig. 4D,E), some relatively sharp cross peaks resonate at positions expected for un-

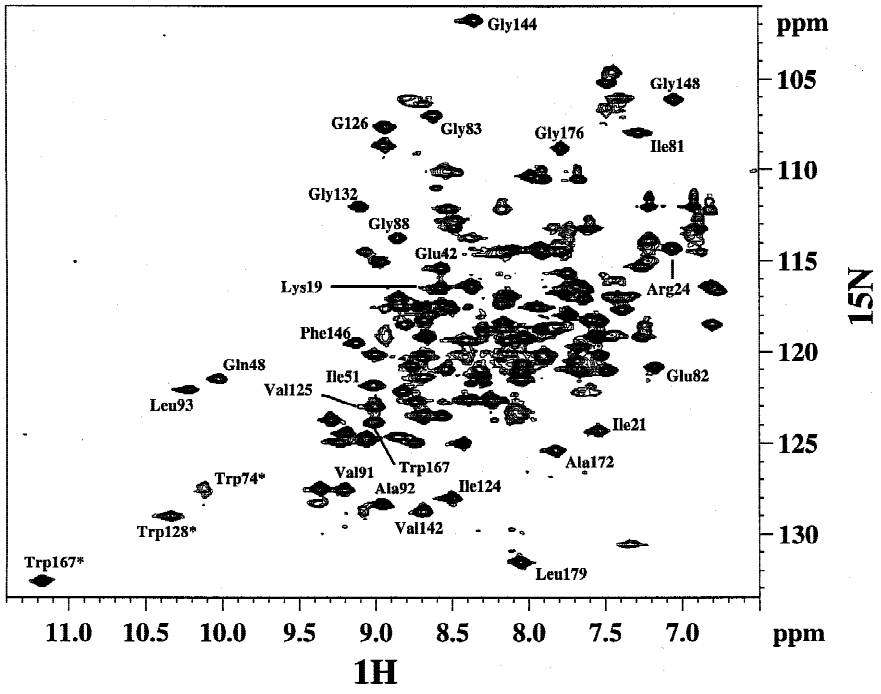

Fig. 3. Gradient-enhanced 500 MHz $^{1}H–^{15}N$ HSQC spectrum of 2.1 mM ^{15}N-labeled native C69A apoflavodoxin from *A. vinelandii*. Indicated are the cross peaks of the residues of which the concentration GndHCl at the midpoint of unfolding (C_m) could be determined in a series of $^{1}H–^{15}N$ HSQC spectra recorded at increasing concentration denaturant. These cross peaks, arising from 25 backbone NH groups, are labeled by residue type and by sequence position. The cross peaks of the indole $N^{\epsilon}H$ groups of Trp74, Trp128, and of Trp167 are indicated by an asterisk. Only positive intensities are shown. The sample contains 100 mM potassium pyrophosphate, 90% H_2O/10% $^{2}H_2O$, at pH 6.0, and the spectrum is recorded at 25 °C. For further details, see Materials and methods.

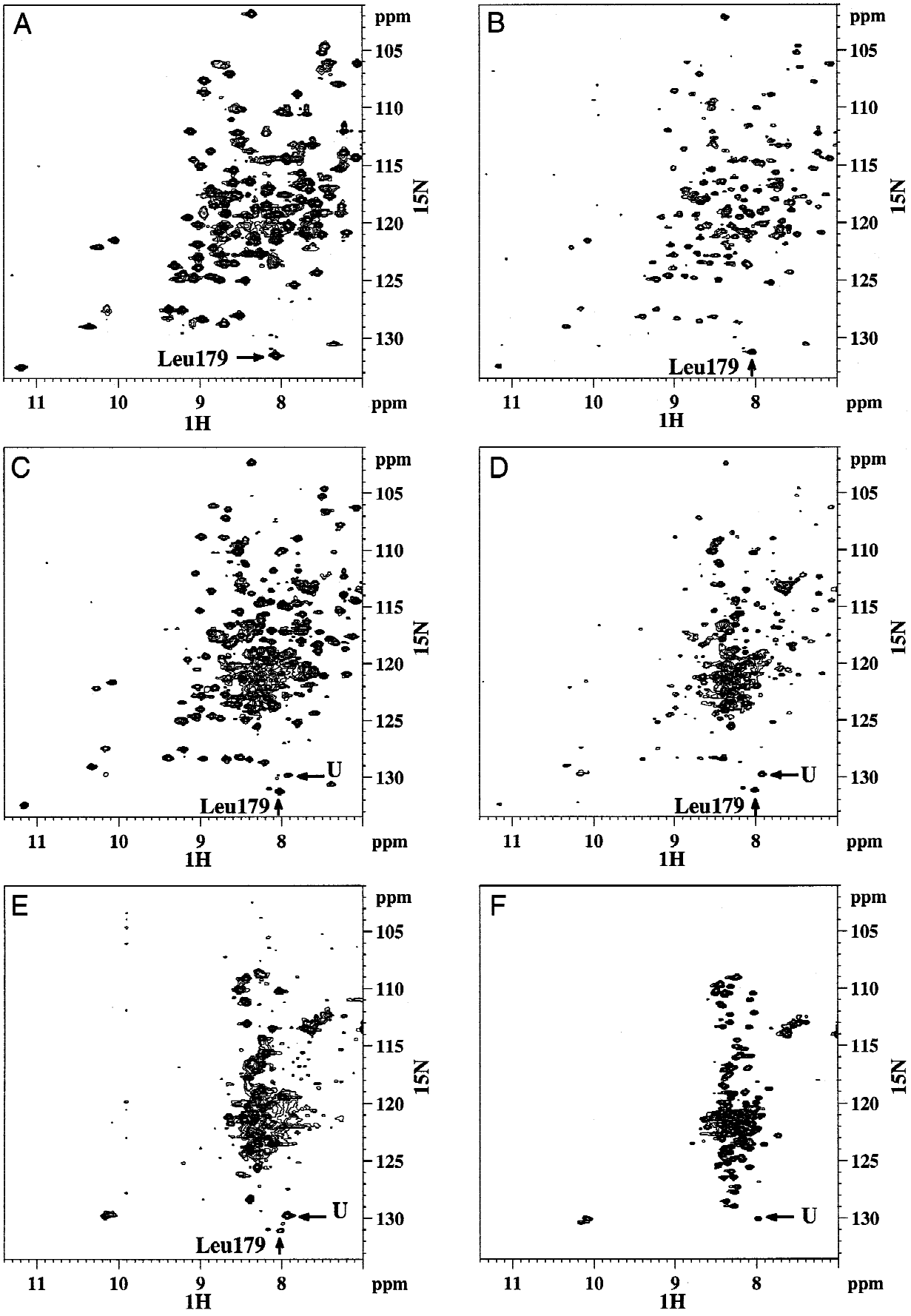
A
B
C
D
E
F
ppm
105
110
115
120
125
130
15N
11
10
9
8
1H
Leu179
U

folded apoflavodoxin (Fig. 4F). The decrease in the cross peak volumes corresponding with native apoflavodoxin continues. Again, the ^{1}H–^{15}N correlations of native apoflavodoxin exhibit relatively small denaturant-concentration-dependent chemical shift changes.

The spectrum acquired in the presence of 4.06 M GndHCl (Fig. 4F) has limited chemical shift dispersion in the ^{1}H dimension and is typical for an unfolded protein. Cross peaks corresponding to amide groups of the same amino acid residue types in the unfolded protein have minimal chemical shift differences; for example, the resonances of the indole NH groups of the three Trp residues of unfolded apoflavodoxin are clustered around (^{1}H = 10.2 ppm, ^{15}N = 131 ppm).

Each addition of a fixed volume of the 5.41 M GndHCl stock solution to the NMR sample volume caused the formation of insoluble apoflavodoxin aggregate, a phenomenon likely to be observed for many other proteins investigated by NMR. The added GndHCl droplet unfolds apoflavodoxin in the immediate mixing area as the initial local concentration denaturant is well above 3 M (Fig. 2). Upon further mixing, the concentration GndHCl drops and apoflavodoxin refolds in the area mentioned. During refolding, a fraction of the apoflavodoxin molecules aggregates. The aggregation is most likely caused by the exposure of hydrophobic groups in the folding intermediates involved, in combination with the relatively high protein concentrations necessary to obtain ^{1}H–^{15}N HSQC spectra with sufficient signal-to-noise ratio. To ensure that the detection area of the NMR probe contained a clear protein solution, the protein aggregate was spinned down to the bottom of the tube prior to the NMR data collection. As a result, deleterious effects due to poor shimming of the sample were avoided. The aggregate did not give rise to any detectable NMR signal in our experiments. At the highest concentration of 4.06 M GndHCl used in our experiments, the aggregate completely dissolved.

Assignment of Leu179 in non-native apoflavodoxin

The assignment of the Leu179 ^{1}H–^{15}N backbone amide correlation of unfolded apoflavodoxin is made possible due to the following observations (Fig. 4). First, the Leu179 ^{15}N resonance is the most low-field shifted nitrogen backbone resonance of the native protein. This is caused by "end group effects" of the deprotonated C-terminal carboxyl group at pH 6.0 on this residue (Bundi & Wüthrich, 1979; Braun et al., 1994). The Leu179 ^{15}N resonance in unfolded apoflavodoxin is most likely, but not necessarily, again the most low-field shifted nitrogen backbone resonance of the protein (Fig. 4F). Second, the backbone amide of this C-terminal residue gives rise to the sharpest cross peak in the ^{1}H–^{15}N HSQC spectra of both native holo- and apoflavodoxin. In addition, the corresponding amide proton exchanges too rapidly to be measured by the hydrogen/deuterium exchange method ($k_{ex} \geq \sim 10^{-2}\ s^{-1}$) (Steensma et al., 1998; Steensma & van Mierlo, 1998). This shows that the C-terminal residue is highly flexible in apo- and holoflavodoxin, as is found for many other proteins. Consequently, only relatively small chemical shift changes of the ^{1}H–^{15}N correlation of the backbone amide of Leu179 are expected upon unfolding of apoflavodoxin (Fig. 4).

In the apoflavodoxin molten globule, the Leu179 nitrogen backbone resonance must be one of the most low-field shifted resonances due to the mentioned "end group effects." However, no obvious candidate cross peak for Leu179 of the apoflavodoxin folding intermediate is observed in the corresponding area of the ^{1}H–^{15}N HSQC spectra. The intermediate species is less structured than native apoflavodoxin, as deduced from tryptophan fluorescence emission spectroscopy studies. We, therefore, infer that the cross peak of the backbone amide of Leu179 in the relatively stable apoflavodoxin folding intermediate coincides with the Leu179 cross peak of fully unfolded apoflavodoxin (see also Discussion).

Correction for the observed apoflavodoxin signal reduction

To correct for dilution and for aggregation upon GndHCl addition, the cross peak volumes of the ^{1}H–^{15}N correlations of the backbone amide of Leu179 were used. They serve as internal markers for the amount of dissolved folded and non-native apoflavodoxin molecules present in the solution. Leu179 was chosen as it is the only residue for which assignments in both folded and non-native states of apoflavodoxin could be deduced.

The correction factor X at a specific concentration denaturant is

$$X(M) = \frac{(V_{\mathrm{Leu179}})_{\text{at 0 M GndHCl}}}{(V_{\mathrm{Leu179}}(\text{native}) + V_{\mathrm{Leu179}}(\text{unfolded}))_{\text{at } X \text{ M GndHCl}}} \quad (1)$$

with V_{Leu179} the cross peak volume of the ^{1}H–^{15}N backbone amide correlation of Leu179 of the initial native apoflavodoxin sample, and $[V_{\mathrm{Leu179}}(\text{native}) + V_{\mathrm{Leu179}}(\text{unfolded})]$ the Leu179 cross peak volumes of native and of unfolded (including intermediate state) apoflavodoxin. The divisor reflects the decreased total amount of apoflavodoxin in solution at a specific concentration of denaturant. Each cross peak volume $V_i(M)$ corresponding with the backbone amide of amino acid residue i at a specific concentration denaturant is multiplied by this correction factor to obtain dilution and aggregation corrected cross peak volumes $V_i^{corr}(M)$:

Fig. 4 (*facing page*)**.** The unfolding of native C69A apoflavodoxin from *A. vinelandii* monitored by signal intensity changes in gradient-enhanced ^{1}H–^{15}N HSQC spectra at different stages during the equilibrium unfolding by guanidinium hydrochloride. The individual two-dimensional (2D) NMR spectra shown here are acquired in the presence of (**A**) 0 M GndHCl, (**B**) 0.99 M GndHCl, (**C**) 1.32 M GndHCl, (**D**) 1.55 M GndHCl, (**E**) 1.75 M GndHCl, and (**F**) 4.06 M GndHCl, respectively. The cross peak resulting from the backbone amide of the C-terminal residue of native apoflavodoxin is labeled Leu179. The corresponding cross peak of Leu179 in unfolded apoflavodoxin is labeled U and is first observed in the ^{1}H–^{15}N HSQC spectrum at 1.32 M GndHCl (**C**). The spectrum acquired in the presence of 4.06 M GndHCl has limited chemical shift dispersion in the ^{1}H dimension and is typical for that of an unfolded protein (van Mierlo et al., 1998). Notice the broadness of several cross peaks in, among others, the region of 7.7–8.5 ppm (^{1}H) and 115–125 ppm (^{15}N) in spectra C, D, and E, which is caused by dynamic exchange between non-native protein conformations on the NMR chemical shift timescale. The six spectra are all contoured at close to the baseline noise level to show as many observable cross peaks as possible. Only positive intensities are shown. The number of scans per individual increment is (**A**) 4, (**B**) 4, (**C**) 64, (**D**) 32, (**E**) 64, and (**F**) 32; for further details, see text and Materials and methods.

$$V_i^{corr}(M) = V_i(M) \cdot X(M). \quad (2)$$

The application of this correction factor has the additional effect that per individual $^1H–^{15}N$ HSQC experiment a proper correction is made for the GndHCl concentration-dependent reduction in the NMR receiver coil quality factor *Q*. Each addition of the denaturant leads to an increased sample conductivity, and thereby reduces *Q*. Whereas adequate sample shimming and receiver coil tuning are easily achieved (Plaxco et al., 1997), the reduction in *Q* leads to a loss in signal intensity of all NMR resonances involved. This denaturant concentration-dependent signal reduction is most easily observed for the water and GndHCl signal in a (90° pulse-acquisition) experiment. A nonlinear relationship between signal-to-noise ratio and concentration GndHCl is observed by us (data not shown). The dependency of the signal-to-noise ratio on the conductivity of the sample corresponds well with the dependency as derived and observed by Kugel (1991). In our NMR setup, the signals are reduced by 42% at 4.06 M GndHCl due to a reduction of *Q*. This is in line with reported values on other NMR spectrometers of 42% at 3.70 M GndHCl (van Nuland et al., 1998) and of 35% at 8 M GndHCl (Plaxco et al., 1997). It is remarkable that, to our knowledge, no GndHCl concentration-dependent intensity correction of NMR unfolding data is made to date, despite the reduction in signal intensity observed. The correction procedure applied by us (Equations 1 and 2) avoids the erroneous determination of folding parameters such as C_m.

Determination of the midpoint of unfolding of individual apoflavodoxin residues

The change in $^1H–^{15}N$ cross peak volume of 35 out of the 154 HSQC cross peaks that were identified by us for native apoflavodoxin (Steensma & van Mierlo, 1998) were followed upon GndHCl-induced unfolding of the protein. In addition, the cross peak corresponding to the $^1H–^{15}N$ correlation of the backbone amide of Leu179 of unfolded apoflavodoxin was tracked. The cross peaks selected are distributed all over the $^1H–^{15}N$ HSQC spectrum and were chosen as they are in isolated positions and do not overlap with other cross peaks. Such overlap would otherwise seriously complicate the analysis of the data. Signals arising exclusively from native apoflavodoxin can thus be followed during the unfolding of the protein. The backbone amide $^1H–^{15}N$ HSQC cross peaks of Leu5, Asp43, Ala45, Gly101, Asp131, Glu134, Glu136, and Val147 were excluded from our analysis due to either overlap with one of the backbone amide cross peaks of the unfolded state in the transition zone of unfolding, or highly scattered cross peak volumes in this zone, or due to low signal-to-noise ratio, resulting in a limited number of data points that are restricted to the native part of the unfolding curve. Figure 5 shows typical examples of the corrected equilibrium unfolding data obtained for various residues of apoflavodoxin.

A two-state mechanism of unfolding in which only native and denatured molecules are taken into account (Pace, 1986) excellently describes the native apoflavodoxin unfolding data as monitored by NMR (Fig. 5). Note that the monitoring of the disappearance of native signals inherently implies a two-state approach in the analysis of unfolding data: i.e., a signal is either present or present with decreased intensity. In a two-state unfolding approach, the free energy of unfolding at zero concentration denaturant, the slope at the midpoint of the unfolding transition, and the concentration guanidinium hydrochloride at the midpoint of unfolding (C_m) can be determined. Of these, the C_m values are generally the most accurately determined. Figure 6 shows the C_m values obtained for the NH groups of various residues of apoflavodoxin using Equation 6.

Differences in cross peak volume dependencies on the concentration denaturant are observed in the native baseline part of the unfolding curves of the various backbone amides (see, for example, the differences between Figs. 5A and 5B). Changes in the rate of exchange of amide protons with water at increasing concentrations denaturant, changes in relaxation behavior in the presence of GndHCl, or more site-specific effects by the interaction of GndHCl could explain these differences (van Nuland et al., 1998). The precise molecular details that cause the differences in the slopes of the native baselines are, however, currently not yet understood.

The $^1H–^{15}N$ backbone amide correlation of Glu82 has only one, and those of Lys19, Arg24, Gly126, Val142, Gly144, and of the indole $N^{\epsilon}H$ of Trp167, have two data points in the transition zone of unfolding. The limited amount of transition zone data points for these residues precludes the accurate determination of C_m values. Consequently, these values, although clustered around the C_m value as obtained by fluorescence spectroscopy (see below), are excluded from our analysis.

The remaining 21 NH groups of native apoflavodoxin that could be tracked over the denaturant range discussed, and of which a reliable C_m value could be determined (Fig. 6), are distributed throughout the whole protein structure (Fig. 7). The C_m values of these NH groups as determined by NMR (scattered around a mean C_m value of 1.48 ± 0.04 M GndHCl) are in close agreement with the C_m value of apoflavodoxin unfolding as measured by relative tryptophan fluorescence at 333 nm (1.54 ± 0.01 M GndHCl) (van Mierlo et al., 1998) (Fig. 6). Clearly, the midpoints of unfolding as determined by both NMR and fluorescence emission spectroscopy do not coincide with the one obtained by CD spectroscopy (C_m is 1.75 ± 0.04 M GndHCl) (van Mierlo et al., 1998) (Fig. 2).

Discussion

Native apoflavodoxin unfolds cooperatively

In the present study, as part of the investigation of how *A. vinelandii* flavodoxin folds, the denaturant-induced equilibrium unfolding of apoflavodoxin as followed by NMR is reported. NH groups of a variety of residues of apoflavodoxin are followed in a series of $^1H–^{15}N$ HSQC spectra recorded at increasing concentrations of guanidinium hydrochloride. These NH groups function as beacons in apoflavodoxin (Fig. 7) and reflect the properties of the molecule during unfolding. The 21 coinciding C_m values (Figs. 6, 7) reflect that all secondary structure elements sampled of apoflavodoxin behave similarly as a function of the concentration GndHCl. This shows that the transition of native apoflavodoxin to its molten globule state is highly cooperative.

Both NMR and fluorescence spectroscopy are highly sensitive to changes in the tertiary structure of the protein caused by denaturant-induced unfolding. The C_m value obtained via fluorescence emission spectroscopy, which informs about changes in the local micro environment of the three tryptophan residues of apoflavodoxin, coincides with the 21 C_m values obtained by NMR including those for Trp74, Trp128, and for Trp167 (Fig. 6). However, these values (average C_m by NMR: 1.48 ± 0.04 M GndHCl; C_m by fluorescence emission spectroscopy: 1.54 ± 0.01 M GndHCl) dif-

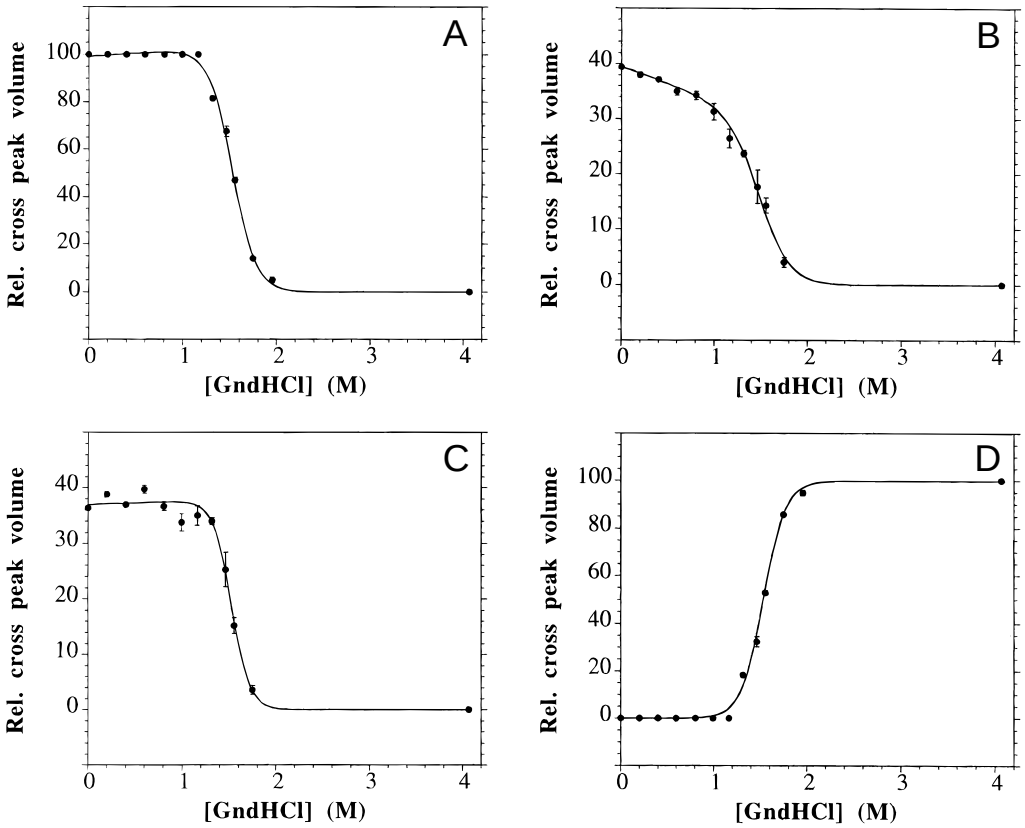

Fig. 5. Denaturant-induced unfolding of C69A apoflavodoxin from *A. vinelandii* as monitored by changes in cross peak volumes in gradient-enhanced $^{1}H–^{15}N$ HSQC spectra at various concentrations guanidinium hydrochloride. The integral of the cross peak volume that corresponds with the backbone amide of Leu179 of native apoflavodoxin at 0 M GndHCl is set to 100. All cross peak volumes are corrected as is described in the text. Shown are the changes in the cross peak volumes of the backbone amides of (**A**) Leu179, (**B**) Trp167, and of (**C**) the indole $N^{\epsilon}H$ group of Trp128 of native apoflavodoxin, and of (**D**) the backbone amide of Leu179 of unfolded apoflavodoxin. The solid curves show the best fit of a two-state model of protein unfolding to the apoflavodoxin unfolding data. This fit is used to extract the corresponding C_m value: (**A**) 1.52 ± 0.01 M, (**B**) 1.50 ± 0.02 M, (**C**) 1.52 ± 0.01, and (**D**) 1.53 ± 0.01 M. The standard deviations of the individual data points are indicated by bars.

fer significantly from the C_m value as measured by CD spectroscopy (1.75 ± 0.04 M GndHCl) (van Mierlo et al., 1998). This confirms that the unfolding of apoflavodoxin does not follow a simple two-state process.

The cross peaks of native apoflavodoxin we checked do not show a detectable increase in cross peak linewidths between 0 and 1.95 M GndHCl (however, the ^{1}H line width of the indole $N^{\epsilon}H$ group of Trp128 decreases). A decrease in cross peak volume and only relatively small, denaturant concentration-dependent, chemical shift changes are observed for native apoflavodoxin upon adding denaturant. Besides an obvious decrease in conformational stability, apparent via the decreasing fraction of native molecules present, the conformational properties of native apoflavodoxin do not change in the transition zone of protein unfolding. The unaltered line widths of native apoflavodoxin imply that the exchange between the native protein and the relatively stable folding intermediate is slow on the NMR chemical shift timescale.

Formation of the apoflavodoxin molten globule

Upon increasing the concentration of denaturant, native apoflavodoxin cooperatively unfolds to a species with molten globule-like properties. The folding intermediate accumulates in the transition zone of the denaturant-induced unfolding of apoflavodoxin (Fig. 2) (van Mierlo et al., 1998). Many cross peaks that are severely broadened in the ^{1}H and ^{15}N dimension are observed in the corresponding $^{1}H–^{15}N$ HSQC spectra (Fig. 4C–E). This broadness is a result of exchange at an intermediate exchange rate on the chemical shift timescale. The exchange is presumably between the relatively stable apoflavodoxin folding intermediate and the unfolded molecules. Conformational fluctuations on a millisecond timescale throughout the apoflavodoxin molten globule state itself, however, might also contribute to the line broadening observed as is proposed for the α-lactalbumin molten globule by Schulman et al. (1997). The severe line broadening excludes the assignment of the vast majority of the NMR resonances of the apoflavodoxin molten globule. The maximum accumulation of the intermediate state of C69A apoflavodoxin at 1.72 M GndHCl is only 22% of the total amount of molecules present (van Mierlo et al., 1998). The additional presence of native state and fully unfolded molecules further complicates the characterization of the apoflavodoxin molten globule state by NMR spectroscopy.

In the transition zone of unfolding (Fig. 4D,E), some relatively sharp cross peaks appear that resonate at positions similar to those

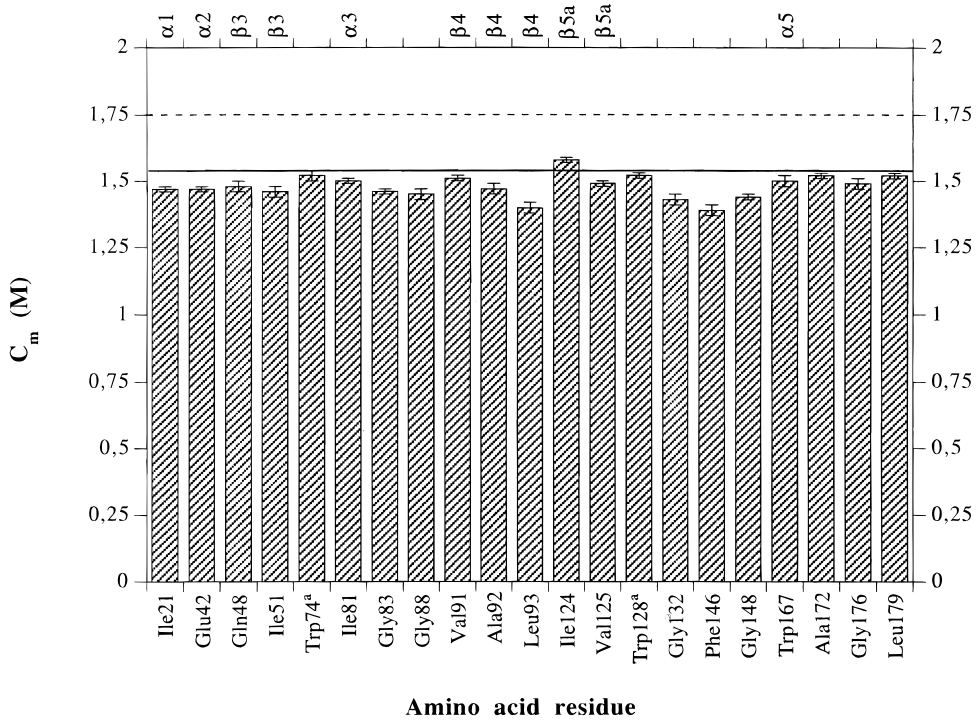

Fig. 6. Concentration guanidinium hydrochloride at the midpoint of unfolding (C_m) as observed by NMR for the backbone NH groups of various residues of native *A. vinelandii* C69A apoflavodoxin. The C_m values and their standard errors are calculated by applying Equation 6 to the integrals of the cross peaks of individual NH groups in a series of ^1H–^{15}N HSQC spectra recorded at increasing concentration denaturant. The solid and the dashed lines show the C_m values as obtained for the apoflavodoxin equilibrium unfolding data as determined by relative tryptophan fluorescence at 333 nm (1.54 ± 0.01 M GndHCl) and by CD in the far ultraviolet (222 nm) (1.75 ± 0.04 M GndHCl), respectively (van Mierlo et al., 1998). Secondary structure elements of apoflavodoxin (Steensma & van Mierlo, 1998) are indicated in the top part of the graph. [a]C_m value is determined for the indole N$^\epsilon$H group of the residue.

observed for unfolded apoflavodoxin (Fig. 4F). The linewidths of these cross peaks in the transition zone, however, are still larger than those observed for fully unfolded apoflavodoxin. The latter is due to exchange at an intermediate exchange rate on the chemical shift timescale between fully unfolded apoflavodoxin molecules and presumably the apoflavodoxin molten globule.

The chemical shift difference between resonances of exchanging species, in addition to the exchange rate, will determine whether a system is in slow, fast, or intermediate exchange on the NMR chemical shift timescale. The chemical shift differences between the resonances of native apoflavodoxin molecules and the corresponding ones of the molten globule state may be larger than the chemical shift differences between the resonances of the molten globule and the corresponding ones of the unfolded states. Therefore, it is possible that exactly the same exchange rates could on the NMR chemical shift timescale give rise to the slow exchange observed for the native to molten globule transition and the intermediate exchange observed for the molten globule to unfolded transition. The presence of the relatively stable molten globule-like species in the denaturant-induced equilibrium (un)folding of apoflavodoxin implies that high-energy transition barriers exist for the formation of this intermediate species. The final transition of the molten globule to the native state of a protein is often the slowest step in folding (Ptitsyn, 1995; Dobson & Karplus, 1999). However, it still remains to be established whether this transition is the slowest step in equilibrium and kinetic folding of apoflavodoxin.

Only a fraction of the total number of cross peaks observed for fully unfolded apoflavodoxin appears in the ^1H–^{15}N HSQC spectra recorded between 1.16 and 1.95 M GndHCl (Fig. 4). This implies that only part of the molten globule unfolds in the denaturant concentration range studied. This finding is highlighted for the glycine residues of apoflavodoxin in Figure 8. The figure shows the region of the ^1H–^{15}N HSQC spectra that contains cross peaks that mainly arise from the backbone amides of the glycine residues of a protein. As can be seen, only a fraction of the 20 expected cross peaks resulting from the backbone amides of the 20 glycine residues of unfolded apoflavodoxin are observed in the transition zone of unfolding. In contrast, the spectrum acquired in the presence of 4.06 M GndHCl shows the expected 20 cross peaks in the region [7.9–8.6 ppm (^1H), 108–114 ppm (^{15}N)] arising from the 20 glycine backbone amides of unfolded apoflavodoxin. These NMR results indicate that the three-state model used to describe the unfolding data presented in Figure 2 is an oversimplification of the actual apoflavodoxin folding process. Whereas the CD data suggest a cooperative unfolding of the molten globule, the NMR data clearly show that this is not the case.

Detection of a reporter group

By using the correction factor (Equation 1), we assume that the Leu179 backbone amide resonances of the apoflavodoxin folding intermediate are sharp and are identical to the ones in the fully unfolded state of the protein. Sharp cross peaks were, for instance,

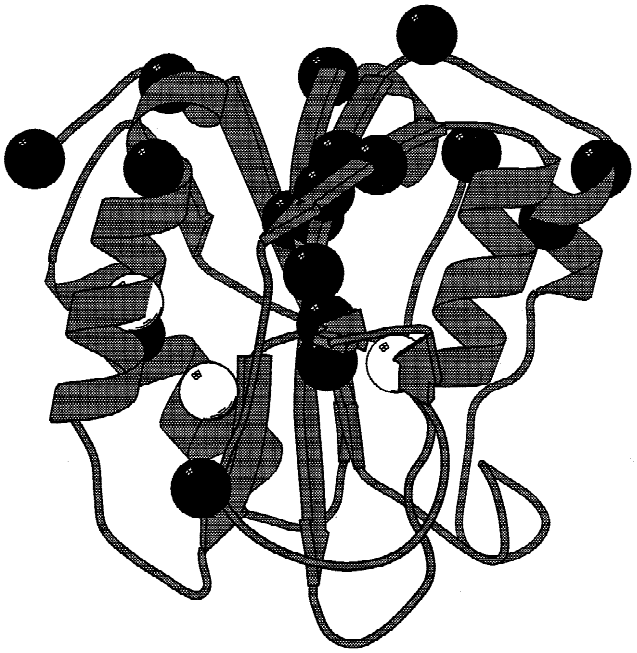

Fig. 7. MOLSCRIPT cartoon drawing (Kraulis, 1991) of the structure of apoflavodoxin (see caption of Fig. 1) in which spheres indicate the NH groups that are followed in a series of ^{1}H–^{15}N HSQC spectra recorded at increasing concentrations of guanidinium hydrochloride. The spheres are drawn with van der Waals radii around the corresponding nitrogen atoms. Black spheres show backbone nitrogen atoms, and white spheres show from left to right: the backbone nitrogen of Trp167, the indole $N^{\epsilon}H$ of Trp128 and of Trp74, respectively. As can be seen, the 21 NH groups are distributed throughout the whole protein structure. The orientation of the apoflavodoxin structure is identical to the one shown in Figure 1.

observed for the flexible N-terminal 15 residues of the (30–51) intermediate in the disulfide folding pathway of bovine pancreatic trypsin inhibitor (BPTI) (van Mierlo et al., 1992a, 1992b). The resonances of many of the backbone amide protons of the folded portion of the (30–51) intermediate, however, were broadened to various extents relative to their counterparts in native BPTI. Similarly, for the human α-lactalbumin molten globule at pH 2.0 and 20 °C, resonances of the three unfolded N-terminal residues that are not spatially restricted by the 6–120 disulfide bond were observed, whereas other resonances of the α-lactalbumin molten globule are broadened beyond detection (Schulman et al., 1997).

It could be possible, however, that the Leu179 backbone amide cross peak of the folding intermediate does not coincide with the one of the fully unfolded protein but instead is not assigned or broadened beyond detection. This would imply that the C_m values reported here would be too high. However, we argue that this is unlikely as the C_m values obtained for the three tryptophan residues by NMR coincide with the C_m value as measured by fluorescence emission spectroscopy (see above).

The aggregation observed after the addition of a highly concentrated GndHCl solution to a protein NMR sample in the millimolar range is a phenomenon that is often encountered. We show for apoflavodoxin, that if a reporter group (here the C-terminal residue Leu179) can be detected by NMR during the different stages of protein unfolding, the NMR unfolding data can be properly corrected for the aggregation observed and analyzed. Such a correction should be applicable as well to other proteins that suffer from aggregation during NMR unfolding experiments.

Conclusion

The residue-specific NMR (un)folding data presented by us show that the unfolding of apoflavodoxin is not a simple two- or three-state process. Native apoflavodoxin is shown to cooperatively unfold to a molten globule-like state with extremely broadened NMR resonances. This unfolding step is slow on the NMR chemical shift timescale. The subsequent unfolding of the molten globule is faster on the NMR chemical shift timescale, and the limited appearance of ^{1}H–^{15}N HSQC cross peaks of unfolded apoflavodoxin indicates that this process is noncooperative. A similar observation has been reported for the human α-lactalbumin molten globule (Schulman et al., 1997). A further characterization at the residue level of the unfolding of the apoflavodoxin molten globule in increasing concentrations of denaturant has to await the complete assignment of the backbone amide resonances of fully unfolded apoflavodoxin. Once that is accomplished, the molecular details of the folding transitions of the apoflavodoxin molten globule will be revealed. The investigations of the folding of flavodoxin, which is an excellent model system to study protein folding, should lead to a better understanding of the fundamental rules that describe the folding of proteins with a flavodoxin-like fold.

Materials and methods

Purification and sample preparation

Uniformly ^{15}N-labeled recombinant *A. vinelandii* (strain ATCC 478) C69A holoflavodoxin II was obtained and purified as described previously (Steensma et al., 1998; van Mierlo et al., 1998). Apoflavodoxin was subsequently prepared by trichloroacetic acid preparation according to a slightly modified version (van Mierlo et al., 1998) of the original procedure described by Edmondson and Tollin (1971).

The native apoflavodoxin sample was brought to 100 mM potassium pyrophosphate, pH 6.0, via gel filtration and subsequently concentrated via ultrafiltration using a filtron microsep centrifugal concentrator. The concentration of apoflavodoxin was determined spectrophotometrically using the molar absorption coefficient of 29 mM^{-1} cm^{-1} at 280 nm (Barman & Tollin, 1972). The 500 μL NMR sample contained 2.1 mM ^{15}N-labeled protein in 90% H_2O/10% $^{2}H_2O$. Internal [2,3-$^{2}H_4$] 3-trimethylsilylpropionate (TSP) was present in minute amounts.

NMR spectroscopy

A temperature series of ^{1}H–^{15}N HSQC spectra of native apoflavodoxin was acquired at 303, 302, 301, 300, 299, and 298 K. The rather limited temperature dependent shifts of the individual cross-peaks in combination with the assignments of the protein at 303 K (Steensma & van Mierlo, 1998) enabled the assignment of the ^{1}H–^{15}N correlations in the HSQC spectrum of apoflavodoxin recorded at 298 K.

Apoflavodoxin was subsequently unfolded in the NMR tube at 298 K by the controlled addition of 5.41 M GndHCl in 100 mM potassium pyrophosphate pH 6.0 in 90% H_2O/10% $^{2}H_2O$. The final protein concentration was 0.52 mM in 4.06 M GndHCl. At each concentration denaturant used, the NMR probe was tuned and matched, the magnet shimmed, and the 90° pulse length adjusted to compensate for the increasing ionic strength upon addition of GndHCl. Subsequently, a (90° pulse-acquisition) experiment was done to determine the water and GndHCl signal. Finally, at each

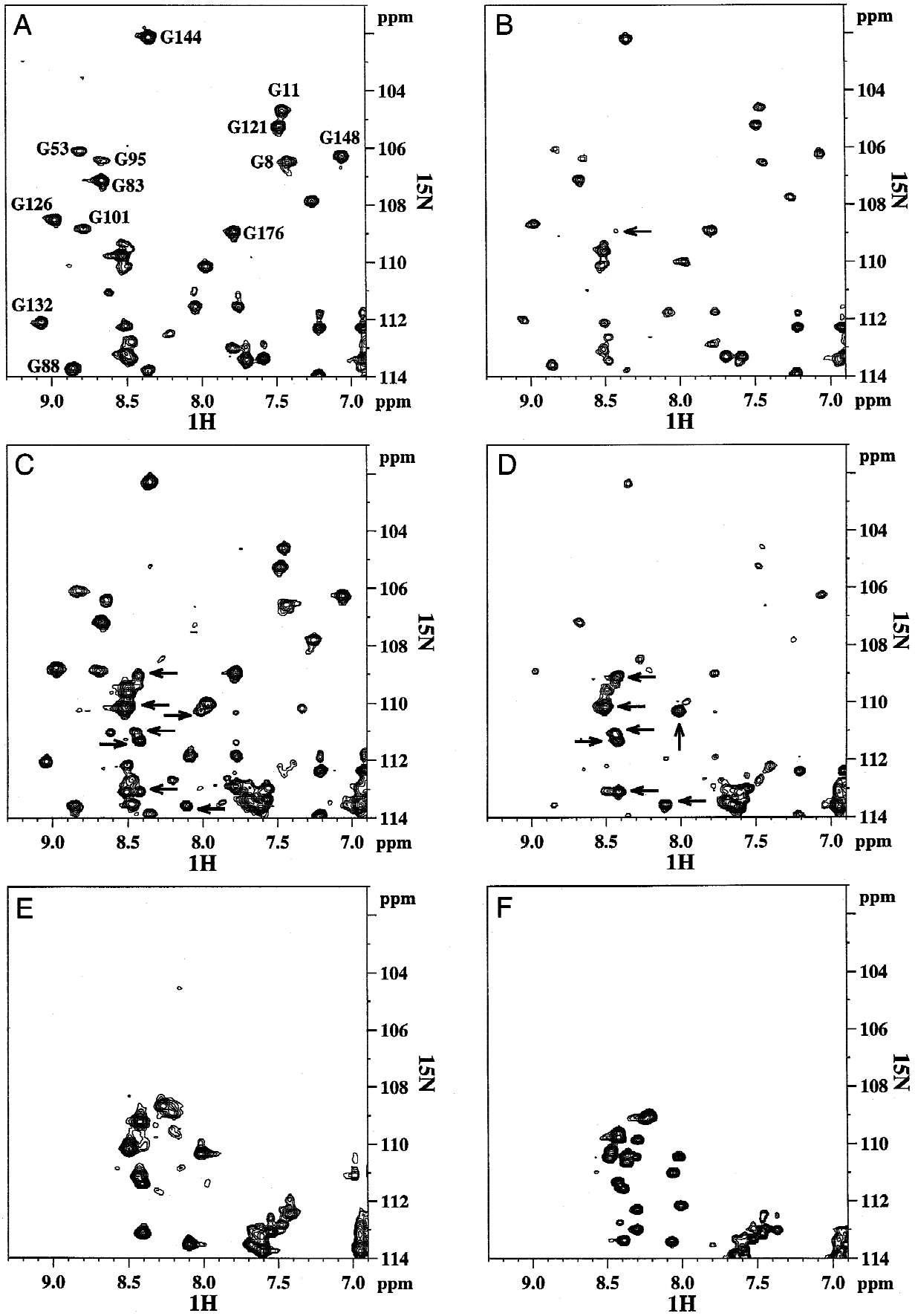
A
G144
G11
G121
G148
G53
G95
G8
G83
G126
G101
G176
G132
G88
B
C
D
E
F
ppm
104
106
108
110
112
114
15N
9.0
8.5
8.0
7.5
7.0
ppm
1H

concentration denaturant used, a $^1H–^{15}N$ HSQC spectrum was recorded.

All gradient-enhanced $^1H–^{15}N$ HSQC spectra (Palmer et al., 1991; Kay et al., 1992) were recorded on a Bruker AMX-500 spectrometer with a triple resonance 5-mm inverse probe with a self-shielded z-gradient. Quadrature detection in the sensitivity enhanced indirect dimension was accomplished by alternate N- and P-type selection (Cavanagh & Rance, 1990; Palmer et al., 1991; Kay et al., 1992). ^{15}N decoupling during acquisition was accomplished using the GARP sequence with a 1.4 kHz rf field strength (Shaka et al., 1985), no water presaturation took place. In the ^1H dimension of the $^1H–^{15}N$ HSQC experiments, 512 complex data points were acquired, whereas in the indirect ^{15}N dimension 256 complex data points were collected. The spectral widths were 8,065 and 1,863 Hz in t_2 and t_1, respectively. With the number of scans set to 4, the experiment lasted 44 min. The number of scans acquired per individual t_1 increment were: 4 at 0.00 and 0.20 M; 32 at 0.40 M; 4 at 0.60, 0.81, 0.99, and 1.16 M; 64 at 1.32 M; 4 at 1.46 M; 32 at 1.55 M; 64 at 1.75 M; and finally 32 at 1.95 and 4.06 M GndHCl, respectively.

Data processing

The NMR data were processed on a Silicon Graphics Indigo II workstation using the XWINNMR version 2.1 software package (Bruker Analytik GmbH, Ettlingen, Germany). The data were apodized using a Gaussian multiplication in t_2 and a 90° shifted sine-bell squared window function in t_1, respectively, zero-filled to obtain a final point-to-point resolution of 2.0 Hz in F_2 and 3.6 Hz in F_1, respectively, and Fourier transformed. The resulting spectra were baseline corrected in the F_2 dimension. The cross peak volumes and changes therein were determined using the integration option in the XWINNMR software package and are used to describe the individual unfolding curves. The ^1H chemical shifts were referenced using internal TSP as a standard and pH–corrected values are shown in the figures in ppm relative to DSS (2,2-dimethyl-2-silapentane-5-sulfonate sodium salt). ^{15}N chemical shifts were referenced indirectly using the consensus Ξ ratio of 0.101329118 (Wishart et al., 1995).

Cross peak volumes instead of cross peak intensities were determined as the viscosity of the solution increases upon addition of GndHCl. On going from 0 to 4 M GndHCl, the viscosity increases by a factor of about 1.27 (Kawahara & Tanford, 1966). As a consequence, the rotational correlation time of apoflavodoxin should decrease and the transverse relaxation times of both the proton and the nitrogen resonance should diminish. Due to these line broadening effects, cross peak intensities are affected, and hence an analysis of cross peak volumes is appropriate. However, between 0 and 1.95 M GndHCl, the highest concentration GndHCl at which any NMR signal arising from native apoflavodoxin was detected, the viscosity of a GndHCl solution increases by only a factor of about 1.09 (Kawahara & Tanford, 1966). The expected increase in cross peak linewidths of about 9% is within the error at which ^1H and ^{15}N linewidths can be determined in our $^1H–^{15}N$ HSQC experiments. In agreement with these considerations, the cross peaks checked, indeed, did not show an increase in cross peak linewidths between 0 and 1.95 M GndHCl (however, the ^1H linewidth of the indole $N^{\epsilon}H$ group of Trp128 decreases).

GndHCl-induced unfolding

The unfolding experiments were done in 100 mM potassium pyrophosphate pH 6.0. A 6 M GndHCl stock solution was prepared gravimetrically in a volumetric flask analogous to the procedure proposed by Pace et al. (Pace, 1986; Pace et al., 1989). Addition of a fixed amount of buffer in 100% ^2H_2O resulted in a 5.41 M GndHCl stock solution in 100 mM potassium pyrophosphate pH 6.0 in 90% H_2O/10% ^2H_2O. This unfolding buffer was added to the NMR tube that contains apoflavodoxin to ensure that the volume percentage of ^2H_2O is maintained at 10% upon unfolding the protein. As a result, among others, the capacity to lock the magnetic field during the NMR experiments remains unaltered.

Desired concentrations of GndHCl were prepared volumetrically: fixed volumes of the GndHCl stock were added to the apoflavodoxin solution by using a Hamilton syringe (Hamilton Bonaduz AG, Bonaduz, Switzerland) followed by thorough mixing. As a check, and to avoid cumulative volume errors, an analytical balance was used to weigh the NMR tube prior to and just after each addition of the denaturant. The mass difference thus known, in combination with the calculated density of the GndHCl stock, enabled the determination of the GndHCl concentration. The volume- and mass-based approach gave essentially identical concentration values. Here, the mass-based values are used.

A blanco series of GndHCl concentrations was made in an NMR tube containing solely buffer in 90% H_2O/10% ^2H_2O. To determine the water and the GndHCl signal (90° pulse-acquisition), NMR experiments were done on this series. The integral of the GndHCl NMR signal as a function of the concentration denaturant obtained for the blanco and for the apoflavodoxin containing solution coincided.

Data analysis

The GndHCl-induced unfolding data as monitored by the disappearance of the NMR signals of native apoflavodoxin could be

Fig. 8 (*facing page*)**.** The unfolding of native C69A apoflavodoxin from *A. vinelandii* monitored by signal intensity changes in gradient-enhanced $^1H–^{15}N$ HSQC spectra at different stages during the equilibrium unfolding by guanidinium hydrochloride. The region of the $^1H–^{15}N$ HSQC spectra shown contains cross peaks that mainly arise from the backbone amides of the glycine residues of a protein. Assigned glycine cross peaks of native apoflavodoxin (Steensma & van Mierlo, 1998) are labeled in spectrum **A**. The individual 2D NMR spectra shown here are acquired in the presence of (**A**) 0.81 M GndHCl, (**B**) 1.16 M GndHCl, (**C**) 1.32 M GndHCl, (**D**) 1.55 M GndHCl, (**E**) 1.95 M GndHCl, and (**F**) 4.06 M GndHCl, respectively. Cross peaks due to unfolded apoflavodoxin are indicated by arrows in spectrum (**B**), (**C**), and (**D**). All cross peaks observed in spectra (**E**) and (**F**) result from unfolded protein. The spectrum acquired in the presence of 4.06 M GndHCl shows the expected 20 cross peaks in the region [7.9–8.6 ppm (^1H), 108–114 ppm (^{15}N)] arising from the 20 glycine backbone amides of unfolded apoflavodoxin. The six spectra are all contoured at close to the baseline noise level to show as many observable cross peaks as possible. Only positive intensities are shown. The number of scans per individual increment is (**A**) 4, (**B**) 4, (**C**) 64, (**D**) 32, (**E**) 32, and (**F**) 32; for further details, see text and Materials and methods.

analyzed according to a two-state model of unfolding in which only the native and the denatured states are populated (Pace, 1986; Pace et al., 1989; Schmid, 1989; 1992). The free energy of unfolding a protein is assumed to be linearly dependent on the denaturant concentration (Pace, 1986):

$$\Delta G_{N\text{-}U} = \Delta G^0_{N\text{-}U} + m[D] \tag{3}$$

with $\Delta G_{N\text{-}U}$ the free energy of unfolding at a particular concentration of denaturant, $\Delta G^0_{N\text{-}U}$ the free energy of unfolding at zero concentration denaturant, m the slope at the midpoint of the unfolding transition, and $[D]$ the concentration of denaturant, respectively. In analogy to Jackson et al. (1993), it follows from the linear dependence of the free energy of unfolding on the denaturant concentration that at C_m: $\Delta G^0_{N\text{-}U} = -m \cdot C_m$; thus

$$\Delta G_{N\text{-}U} = m([D] - C_m). \tag{4}$$

Incorporation of this identity into the linear extrapolation method, which takes into account the linear dependence of the pre- and post-unfolding data on denaturant concentration as proposed by Santoro and Bolen (1988), leads to a general equation that can be fitted to the entire data to determine C_m:

$$Y_{obs} = \frac{(\alpha_N + \beta_N[D]) + (\alpha_U + \beta_U[D])\exp\{-[m([D] - C_m)/RT]\}}{1 + \exp\{-[m([D] - C_m)/RT]\}} \tag{5}$$

with Y_{obs} any physical parameter that characterizes the folded and unfolded states of a protein at a particular concentration denaturant, α and β the intercepts and slopes of the pre- and post-unfolding regimes, and RT is 0.59 kcal mol^{-1}.

In case of the denaturant-induced ^{1}H–^{15}N HSQC apoflavodoxin unfolding data, cross peaks that solely correspond with the native state of the protein were followed. As there is no interference of the final 21 selected cross peaks with those arising from non-native states of the protein, α_U and β_U can be set to zero in Equation 5, resulting in:

$$Y_{obs} = \frac{(\alpha_N + \beta_N[D])}{1 + \exp\{-[m([D] - C_m)/RT]\}}. \tag{6}$$

The C_m values were calculated by applying Equation 6 to the corrected cross peak volumes $V_i^{corr}(M)$ of individual NH groups of native apoflavodoxin in a series of ^{1}H–^{15}N HSQC spectra recorded at increasing concentration denaturant. Equation 5 with α_N, β_N, and β_U set to zero and α_U set to 100 was used to fit to the corrected cross peak volumes of Leu179 in unfolded apoflavodoxin.

Equations 5 and 6 were fitted to the data by nonlinear, least-squares analysis using the general curve fit option of the Kaleidagraph program (version 2.1, Synergy Software, PCS Inc., Reading, Pennsylvania) to obtain values for C_m and their respective standard errors. The individual cross peak volumes $V_i^{corr}(M)$ were weighted during the fit procedure by their corresponding standard deviations. The standard deviations of individual cross peak volumes $V_i(M)$ are determined by the noise in each ^{1}H–^{15}N HSQC spectrum. Subsequently, using Equations 1 and 2, the standard deviation of $V_i^{corr}(M)$ was calculated.

Acknowledgments

We thank Yves J.M. Bollen and Drs. Willem J.H. van Berkel and Walter M.A.M. van Dongen for critical reading of the manuscript.

References

Barman BG, Tollin G. 1972. Flavine-protein interactions in flavoenzymes. Temperature-jump and stopped-flow studies of flavine analog binding to the apoprotein of *Azotobacter* flavodoxin. *Biochemistry 11*:4746–4754.

Braun D, Wider G, Wüthrich K. 1994. Sequence-corrected ^{15}N "random coil" chemical shifts. *J Am Chem Soc 116*:8466–8469.

Brenner SE. 1997. Population statistics of protein structures: Lessons from structural classifications. *Curr Opin Struct Biol 7*:369–376.

Bundi A, Wüthrich K. 1979. Use of amide ^{1}H-NMR titration shifts for studies of polypeptide conformation. *Biopolymers 18*:299–311.

Cavanagh J, Rance M. 1990. Sensitivity improvement in isotropic mixing (TOCSY) experiments. *J Magn Reson 88*:72–85.

Dobson C, Karplus M. 1999. The fundamentals of protein folding: Bringing together theory and experiment. *Curr Opin Struct Biol 9*:92–101.

Edmondson DE, Tollin G. 1971. Chemical and physical characterization of the Shethna flavoprotein and apoprotein and kinetics and thermodynamics of flavin analog binding to the apoprotein. *Biochemistry 10*:124–132.

Jackson SE, Moracci M, elMasry N, Johnson CM, Fersht AR. 1993. Effect of cavity-creating mutations in the hydrophobic core of chymotrypsin inhibitor 2. *Biochemistry 32*:11259–11269.

Kawahara K, Tanford C. 1966. Viscosity and density of aqueous solutions of urea and guanidinium hydrochloride. *J Biol Chem 241*:3228–3232.

Kay LE, Keifer P, Saarinen T. 1992. Pure absorption gradient enhanced heteronuclear single quantum correlation spectroscopy with improved sensitivity. *J Am Chem Soc 114*:10663–10665.

Kraulis PJ. 1991. MOLSCRIPT: A program to produce both detailed and schematic plots of protein structures. *J Appl Crystallogr 24*:946–950.

Kugel H. 1991. Improving the signal-to-noise ratio of NMR signals by reduction of inductive losses. *J Magn Reson 91*:179–185.

Mayhew SG, Tollin G. 1992. General properties of flavodoxins. In: Müller F, ed. *Chemistry and biochemistry of flavoenzymes*, vol. 3. Boca Raton, Florida: CRC Press. pp 389–426.

Pace CN. 1986. Determination and analysis of urea and guanidine hydrochloride denaturation curves. *Methods Enzymol 131*:266–280.

Pace CN, Shirley BA, Thomson JA. 1989. Measuring the conformational stability of a protein. In: Creighton TE, eds. *Protein structure: A practical approach*. Oxford, UK: IRL Press. pp 311–330.

Palmer AG III, Cavanagh J, Wright PE, Rance M. 1991. Sensitivity improvement in proton-detected two-dimensional heteronuclear correlation NMR spectroscopy. *J Magn Reson 93*:151–170.

Plaxco KW, Morton CJ, Grimshaw SB, Jones JA, Pitkeathly M, Campbell ID, Dobson CM. 1997. The effects of guanidine hydrochloride on the "random coil" conformations and NMR chemical shifts of the peptide series GGXGG. *J Biom NMR 10*:221–230.

Ptitsyn OB. 1992. The molten globule state. In: Creighton TE, ed. *Protein folding*. New York: W.H. Freeman and Company. pp 243–300.

Ptitsyn OB. 1995. Molten globule and protein folding. *Adv Protein Chem 47*:83–229.

Santoro MM, Bolen DW. 1988. Unfolding free energy changes determined by the linear extrapolation method. 1. Unfolding of phenylmethanesulfonyl α-chymotrypsin using different denaturants. *Biochemistry 27*:8063–8068.

Schmid FX. 1989. Spectral methods of characterizing protein conformation and conformational changes. In: Creighton TE, ed. *Protein structure: A practical approach*. Oxford, UK: IRL Press. pp 251–285.

Schmid FX. 1992. Kinetics of unfolding and refolding of single-domain proteins. In: Creighton TE, ed. *Protein folding*. New York: W.H. Freeman and Company. pp 197–241.

Schulman BA, Kim PS, Dobson CM, Redfield C. 1997. A residue specific NMR view of the non cooperative unfolding of a molten globule. *Nat Struct Biol 4*:630–634.

Shaka AJ, Barker PB, Freeman R. 1985. Computer-optimized decoupling scheme for wideband applications and low-level operation. *J Magn Reson 64*:547–552.

Steensma E, Heering HA, Hagen WR, van Mierlo CPM. 1996. Redox properties of wild-type, Cys69Ala, and Cys69Ser *Azotobacter vinelandii* flavodoxin II as measured by cyclic voltammetry and EPR spectroscopy. *Eur J Biochem 235*:167–172.

Steensma E, Nijman MJM, Bollen YJM, de Jager PA, van den Berg WAM, van Dongen WMAM, van Mierlo CPM. 1998. Apparent local stability of the secondary structure of *Azotobacter vinelandii* holoflavodoxin II as probed by hydrogen exchange: Implications for redox potential regulation and flavodoxin folding. *Protein Sci 7*:306–317.

Steensma E, van Mierlo CPM. 1998. Structural characterisation of apoflavodoxin shows that the location of the most stable nucleus differs among proteins with a flavodoxin-like topology. *J Mol Biol 282*:653–666.

Tanaka M, Haniu M, Yasunobu KT, Yoch DC. 1977. Complete amino acid sequence of azotoflavin, a flavodoxin from *Azotobacter vinelandii*. *Biochemistry 16*:3525–3537.

Thorneley RNF, Ashby GA, Drummond MH, Eady RR, Hughes DL, Ford G, Harrison PM, Shaw A, Robson RL, Kazlauskaite J, Hill HAO. 1994. Flavodoxins and nitrogen fixation—Structure, electrochemistry and post-translational modification by coenzyme A. In: Yagi K, ed. *Flavins and flavoproteins 1993*. Berlin: Walter de Gruyter & Co. pp 343–354.

van Mierlo CPM, Darby NJ, Creighton TE. 1992a. The partially folded conformation of the Cys30–Cys51 intermediate in the disulfide folding pathway of bovine pancreatic trypsin inhibitor. *Proc Natl Acad Sci USA 89*:6775–6779.

van Mierlo CPM, Darby NJ, Keeler J, Neuhaus D, Creighton TE. 1992b. Partially folded conformation of the (30–51) intermediate in the disulfide folding pathway of bovine pancreatic trypsin inhibitor: ^{1}H and ^{15}N resonance assignments and determination of backbone dynamics from ^{15}N relaxation measurements. *J Mol Biol 229*:1125–1146.

van Mierlo CPM, Lijnzaad P, Vervoort J, Müller F, Berendsen HJC, de Vlieg J. 1990a. Tertiary structure of two-electron reduced *Megasphaera elsdenii* flavodoxin and some implications, as determined by two-dimensional ^{1}H-NMR and restrained molecular dynamics. *Eur J Biochem 194*:185–198.

van Mierlo CPM, Vervoort J, Müller F, Bacher A. 1990b. A two-dimensional ^{1}H NMR study on *Megasphaera elsdenii* flavodoxin in the reduced state: Sequential assignments. *Eur J Biochem 187*:521–541.

van Mierlo CPM, Steensma E. 1999. Stabilisation centres differ between structurally homologous proteins as shown by NMR spectroscopy. *J Mol Cat B: Enzymatic 7*:147–156.

van Mierlo CPM, Steensma E, van Dongen WMAM, van Berkel WJH. 1997. NMR studies on apoflavodoxin II from *Azotobacter vinelandii*. In: Stevenson KJ, Massey V, Williams CH Jr, eds. *Flavins and flavoproteins 1996*. Calgary, Canada: University of Calgary Press. pp 449–452.

van Mierlo CPM, van Dongen WMAM, Vergeldt F, van Berkel WJH, Steensma E. 1998. The equilibrium unfolding of *Azotobacter vinelandii* apoflavodoxin II occurs via a relatively stable folding intermediate. *Protein Sci 7*:2331–2344.

van Nuland NAJ, Meijberg W, Warner J, Forge V, Scheek RM, Robillard GT, Dobson CM. 1998. Slow cooperative folding of a small globular protein HPr. *Biochemistry 37*:622–637.

Wijmenga SS, Steensma E, van Mierlo CPM. 1997. Doubly sensitivity-enhanced 3D HCCH-TOCSY of ^{13}C-labeled proteins in H_2O using heteronuclear cross polarization and pulsed field gradients. *J Magn Reson 124*:459–467.

Wijmenga SS, van Mierlo CPM, Steensma E. 1996. Doubly sensitivity-enhanced 3D TOCSY-HSQC. *J Biomol NMR 8*:319–330.

Wishart DS, Bigam CG, Yao J, Abildgaard F, Dyson HJ, Oldfield E, Markley JL, Sykes BD. 1995. ^{1}H, ^{13}C, and ^{15}N chemical shift referencing in biomolecular NMR. *J Biomol NMR 6*:135–140.